Image Cover Sheet

96-03300

CLASSIFICATION	SYSTEM NUMBER
UNCLASSIFIED	499874

TITLE

NAROWBAND TECHNOLOGIES FOR TACTICAL COMMUNICATIONS

System Number:

Patron Number:

Requester:

Notes:

DSIS Use only:

Deliver to:

Industry
Canada
CRC

NARROWBAND TECHNOLOGIES FOR TACTICAL COMMUNICATIONS (U)

by

**Daniel Boudreau, Yves Jolly,
Pascal Benoit and Luc Boucher**

CRC REPORT NO. 95-005

June 1995
Ottawa

Industry Canada Industrie Canada

The work described in this document was sponsored by the Department of National Defence under Task DFSM002

Canada

Narrowband Technologies for Tactical Communications (U)

by

Daniel Boudreau and Pascal Benoit
Mobile and Personal Communications

Yves Jolly and Luc Boucher
Radiocommunications Technologies Research

The work described in this document was sponsored by the Department of National Defence under Task DFSM002.

COMMUNICATION RESEARCH CENTRE, INDUSTRY CANADA
CRC REPORT NO. 95-005

Canada

June 1996
Ottawa

Abstract

Over the last few decades, mobile radios have been designed for the transmission of uncompressed or slightly compressed voice signals, using frequency modulation in a 25 to 30 kHz channel bandwidth. As the technology evolves, there is a constant trend toward the use of digital voice and modulation methods, in order to reduce the required channel bandwidth and transmitted power for a given voice quality. The objective of this task was the development and the implementation of a state-of-the-art mobile digital narrowband radio.

The ultimate aim is to reduce the use of system resources, such as the required channel bandwidth or the transmitted signal power, as well as the cost of the radio terminals, and to increase the quality of the voice transmission. In order to accommodate such conflicting requirements, sophisticated signal processing techniques are required in both the transmitter and the receiver. Such techniques include: combined source and channel coding, efficient adaptive equalization on fading channels, soft-output symbol detection and combined channel and source decoding. The design of a narrowband radio, making use of some of these advanced techniques, is presented in this report.

Sommaire

Au cours des dernières décennies, différents types d'appareil radios furent conçus pour la transmission de signaux vocaux, sous forme non-compressée, ou légèrement compressée. La modulation en fréquence est, et a été utilisée dans ces appareils, en vue de transmettre sur un canal de largeur de bande de 25 ou 30 kHz. Au fur et à mesure que la technologie évolue, il y a une tendance constante à utiliser des méthodes numériques de compression de la voix et de modulation. Ceci permet de réduire la largeur de bande requise et la puissance de transmission pour une qualité vocale donnée. L'objectif de ce projet était le développment d'un appareil radio numérique à la fine pointe de la technologie.

Le but ultime d'un tel projet est de réduire au minimum la largeur de bande requise, la puissance radio transmise, ainsi que le coût total de l'appareil, tout en améliorant la qualité du signal vocal reçu. Pour accommoder de telles spécifications contradictoires, des techniques sophistiquées de traitement de signal doivent être utilisées, au transmetteur comme au récepteur. Parmi ces techniques, on retrouve: le codage combiné de source et de canal, l'égalisation adaptative sur canaux avec évanouissement, la détection de symbôles quantisés finement et le décodage combiné de source et de canal. La conception d'un tel appareil radio, utilisant certaines de ces techniques de pointe, est présentée dans ce rapport.

Executive Summary

The fundamental building blocks of an implementation of a narrowband mobile radio, using state-of-the-art signal processing algorithms, are presented.

The radio utilizes low bit rate vocoder techniques and bandwidth efficient digital modulation methods.

In order to accommodate challenging design requirements, such as reduced RF channel bandwidth, increased robustness, low transmitted power, and good voice quality, sophisticated signal processing techniques were utilized.

The techniques used in the implementation include combined source and channel coding, efficient adaptive equalization on fading channels, soft-output symbol detection, and combined channel and source coding/decoding. The relationship between the different algorithms is described.

These methods, although computationally extensive, have led to a very effective narrowband mobile radio transmission scheme.

A prototype radio has been built and tested in real time, under laboratory conditions.

It is believed that this radio is one of the most advanced of its kind, and that it is a precursor for future generations of mobile radios.

Contents

List of Figures

List of Tables

1 Introduction

The use of digital signal processing (DSP) techniques in the design of communication systems has become a standard practice. Thanks to the constant increase in the computing power of the DSP microprocessors, today's radios are able to cope with more and more stringent channel conditions, using less and less of the power and spectral resources.

In this report, the design of a narrowband radio capable of transmitting 4.8 kbps in a 6.25 kHz mobile channel is presented. The basic voice data rate is 2400 bps. Error correction capability is provided by adding 1200 bps, and 1200 bps are reserved for the transmission of networking information, encryption, synchronization, etc. The theory behind all the algorithms used in the modulator-demodulator (modem) is presented, and a description of the other peripheral devices, such as the voice coding algorithm, is given. Possible advances in some of the modem functions are presented. They constitute current areas of research, and could be implemented in a future radio version.

In the present document, the radio design specifications are first presented in Section 2. The transmitter is then discussed in Section 3. The voice coding method, the channel coding technique, as well as the modulation format, are covered in that section. The receiver design is addressed in Section 4, where the acquisition, the symbol detection and the channel decoding algorithms are presented. Advances and new research areas are presented in Section 5, in which some improvements over the first prototype implementation are discussed. These more advanced techniques could be implemented in a subsequent project phase. A non-exhaustive set of performance tests and a conclusion are given in the last two sections.

Note that the actual radio hardware and software implementations are not discussed in the present report. These more *practical* considerations are presented in great details in a separate report [1].

2 Specifications

The original system design specifications were:

- Channel bandwidth of 6.25 kHz for half-duplex transmission
- Channel bit rate of 4.8 kbps (encryptable)
- Vocoder rate of 2.4 kbps
- Constant envelope modulation (e.g., Continuous Phase Modulation or CPM)

The channel bandwidth and bit rate were inspired from the North American public safety communications (Project 25) specifications [2]. These specifications are, for the first phase of the Project 25, 12.5 kHz for the channel bandwidth, and 9.6 kbps for the channel bit rate. The radio implementation described in this report is therefore "narrowband" in the sense that it uses half the spectral resources required by the Project 25 specifications, as well as half the bandwidth used by most of the new mobile digital radio services.

Since error correction coding is needed in a mobile environment, the design specification of 4800 bps limits the source coding rate to a value in the order of 4000 bps. A value of 2400 bps for voice coding allows a good compromise between voice quality, error correction requirements and the provision of extra capacity for future use. The constant envelope modulation choice is also inspired from the Project 25 specifications, as well as from the difficulty to obtain a very efficient linear power amplifier (needed, should a linear modulation method be selected). A 4-level continuous phase modulation signal is used in this project, with the phase pulse shape defined as in the Project 25.

3 Transmitter

A high level transmitter block diagram is shown in Fig. 1. It is first composed of a source coder, which encompasses the processes of input speech sampling and source rate compression. Channel coding refers to the addition of controlled redundancy for channel error correction. A multiplexer (MUX) allows a mixing of the voice-related data with other information. Bit interleaving allows, after the corresponding de-interleaving at the receiver, a less correlated sequence of received bits. The 4-level mapper produces, from a given pair of bits, a unique 4-ary symbol. Continuous phase modulation, with the proper phase pulse, is then used to convert the sequence of symbols for channel transmission. The modulated signal may come from three different paths: the *information-related* path, which produces a sequence of varying length, the *preamble* path, which generates a fixed length unique sequence of modulated symbols, used for the receiver synchronization, and the *postamble* path, which also gives a unique sequence, indicating the end of transmission to the receiver. Although not shown in Fig. 1, the modulated sequence is then passed through a digital-to-analog converter, up-converted to RF and transmitted.

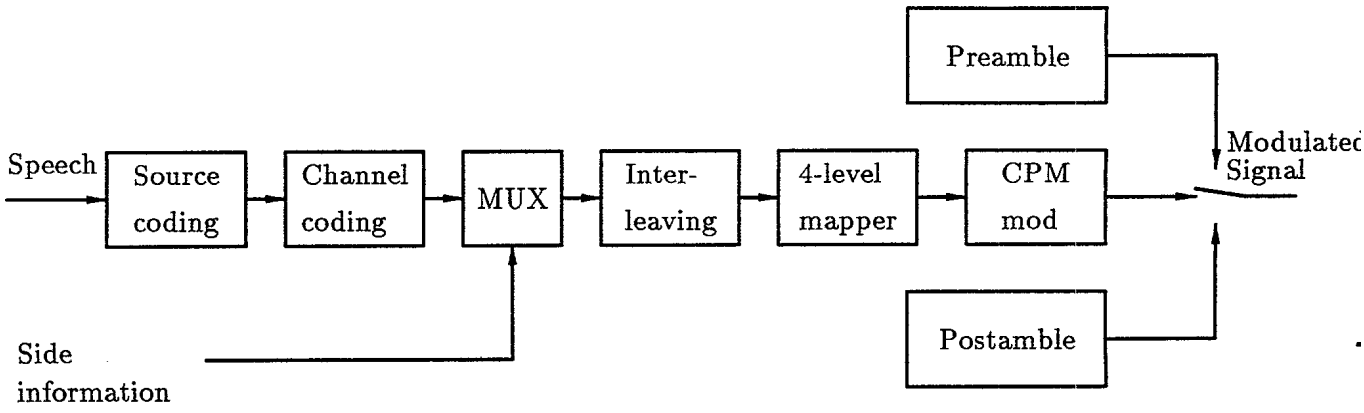

Fig. 1: Transmitter block diagram.

3.1 Source Coding Algorithm

The speech signal is encoded into a 2400 bps digital data stream. The source coding algorithm is a variant of the Improved Multi Band Excitation method of Hardwick and Lim [3]. This new method has been developed at CRC and is called *Frequency Selective Harmonic Coding* (FSHC) [4]. It is a combination of the Multi Band Excitation (MBE) method, where the voice segment spectrum is divided into bands for which a separate voiced/unvoiced decision is taken, and Dynamic Frequency Band Extraction (DFBE), where the perceptually significant spectral bands are extracted. Using this technique, a good quality speech coder has been implemented in real-time hardware, with a bit rate of 2400 bps [5].

As with other forms of voice coding, the input speech is segmented into 20 msec frames. At the 2400 bps rate, each frame represents 48 bits. The bit allocation, depending on the type of frame (voiced or unvoiced) is given in Table 1.

Parameter	Voiced Frames	Unvoiced Frames
Fundamental frequency	8	8
Energy	5	5
Position vector of frequency windows	5	
Energy shape factor	3	
Voicing decision of each frequency window	4	
Spectral amplitudes	22	14
Unused	1	21
Total	48	48

Table 1: Bit allocation of the 2.4 kpbs FSHC vocoder.

For a voiced frame, five frequency windows are used to isolate the most pertinent spectral information of the harmonic spectrum. These five frequency windows span approximately 60% of the spectrum bandwidth. A vector is used to indicate the positions of the windows, from among a predetermined list of allowable ones. A voicing decision for each frequency window is also transmitted. The spectral amplitudes are encoded using a "gain shape" vector quantization scheme, in which a single frame energy parameter is used for the gain factor, and 5 different codebooks, one for each window, is used to encode the spectral shape. The fundamental frequency is also encoded and transmitted. The 48th bit is free and can be used to send an alternating frame synchronization bit.

For an unvoiced frame, only 2 fixed frequency windows are used to span the entire harmonic spectrum. No position vector is required. To indicate that the encoded frame is unvoiced, the 8 bits

of the fundamental frequency parameter are all set to one (a very unlikely value for a voiced frame). The spectral amplitudes are again encoded using a "gain shape" vector quantization scheme, with a different codebook for each frequency band. The fundamental frequency is not transmitted, since a fixed value is always used to generate the harmonic spectrum. An alternating frame synchronization bit can again be included. Only 27 of the 48 frame bits are currently used to encode the model parameters for an unvoiced frame.

3.2 Channel Coding Algorithm

The source data stream is then processed by the channel coding algorithm. In order to be most effective, the channel coding must be adapted to the statistics of the source coded symbols, as well as to the channel conditions. The source and channel coding techniques should be combined in such a way that the most perceptually sensitive source parameters are the most protected from channel errors. Ultimately, the source bits and the channel coding bits should be distributed according to the channel conditions: more channel coding should be utilized in bad conditions, and more elaborate source coding selected in good ones.

In the radio system designed in this project, the bit distribution is fixed and has been determined from a perceptual analysis of the source parameters in different channel conditions. In order to allow variable protection, rate compatible punctured convolutional (RCPC) codes are used for channel coding [6]. This form of channel coding allows the use of a single channel coder with a single maximum likelihood decoder (Viterbi decoder). By dropping some of the convolutional encoder outputs in a controlled manner, the effective rate of a given code (the mother code) can be increased from its basic value. Since the code trellis does not change, except for some outputs that are not transmitted, the same maximum likelihood decoder can be used for every possible rate. The choice of the puncturing rule is governed by the need for a smooth bit error probability performance in the transition from one rate to the other. This is assured by the *compatibility* rule of the RCPC code. This rule essentially states that, in going from a higher rate punctured code to a lower rate one, all the output symbols of the former are used by the latter. Therefore, all high rate codes are embedded into the lower rate codes and the encoder uses the same shift register for all code rates.

The channel code is designed by grouping the 48 bits, generated by the source encoder during each 20 msec frame interval, into subgroups with similar channel sensitivities. Subjective listening tests allowed the grouping of the frame bits into three categories: *very sensitive*, *sensitive* and *almost not sensitive*. The test of a particular bit consisted in the modulo 2 addition of a one to this bit, thereby creating an error, and listening to the corresponding recovered speech. A number of speech sequences, for both female and male speakers, were tested. Of the 48 bits, eight were found to be very sensitive. Four of these highly sensitive bits correspond to the four most significant bits (MSB) used to encode the frame energy, while the others correspond to the four MSB of the fundamental frequency parameter. Sixteen bits were considered sensitive, and correspond in general to some of the MSB of the other parameters. Finally, the remaining 24 bits were found not to be very affected by single channel errors.

The channel data rate being 4800 bps, 96 bits are transmitted on the channel for each 20

msec frame. The amount of channel coding redundancy was chosen to be 1200 bps, giving an average coding rate of $2/3$. A voice frame will therefore be coded into 72 channel bits by the RCPC coder. The choice of this coder must take into account the compatibility rule, and must give a non catastrophic family of codes. Considering the work of Hagenauer [6], a rate=$1/3$, constraint length=5 convolutional code, with the generator matrix given by (in octal form)

$$G = \begin{bmatrix} 2 & 3 \\ 3 & 5 \\ 2 & 7 \end{bmatrix}, \tag{1}$$

was chosen as the mother code. With a puncturing period of 8 input bits (i.e. the period at which the puncturing process repeats), this code allows the family of coding rates shown in Table 2.

Number of punctured bits	0	2	4	6	8	10	12	14	15	16
input bits/output punctured bits	$8/24$	$8/22$	$8/20$	$8/18$	$8/16$	$8/14$	$8/12$	$8/10$	$8/9$	$8/8$
Corresponding rate	$1/3$	$4/11$	$4/10$	$4/9$	$1/2$	$4/7$	$2/3$	$4/5$	$8/9$	1

Table 2: Some of the possible punctured rates.

This family of codes is well suited to encode the 48 frame bits, since the mother code at rate $1/3$ can be used to encode the 8 most sensitive bits, the $2/3$ punctured code can process the 16 medium sensitivity bits and the unsensitive bits can be transmitted without coding. This gives 72 coded channel bits, as shown in Table 3.

Sensitivity level	Number of input bits	Code rate	Number of output bits
Low	24	1	24
Medium	16	$2/3$	24
High	8	$1/3$	24
Total	48		72

Table 3: The coded channel bits allocation.

This bit allocation is performed with the encoder described in Fig. 2. The encoder operates with a period of 48 input bits. It is assumed that the first 24 input bits arriving at the encoder are the *low* sensitivity ones, that the following 16 input bits correspond to the *medium* sensitivity ones and that the remaining 8 incoming bits are those to be encoded the most heavily. The *level 1* output bits are therefore not coded and are passed directly to the output, without entering the

coder memory. The *level 2* output bits are the 2/3 coded bits and are alternatively obtained from the B and C outputs; except when a "0" appears in the puncturing tables. The *level 3* output bits are the 1/3 coded bits and are the mother code output without puncturing.

In order to allow time independence between the channel coded vocoder frames, 4 *zero* bits are input to the channel coder, after the 48th input frame bit. These bits serve the purpose of resetting the channel coder, such that the next frame will start in a known state. The four zero bits are encoded in 12 channel bits and are transmitted after the 72 RCPC bits. This leaves 12 bits per frame (600 bps) for the transmission of side information.

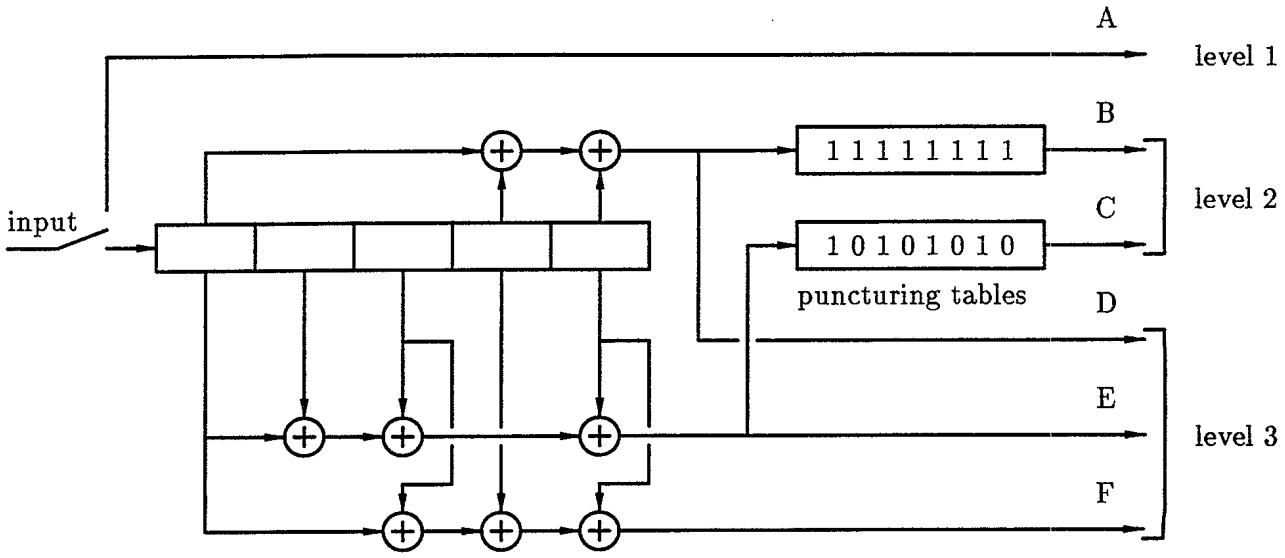

Fig. 2: The RCPC coder. A zero in the puncturing table means *no output.*

3.3 Multiplexer

The following block shown in the transmitter implementation (Fig. 1) is a multiplexer, used to mix some extra information with the channel coded bits. The rate of this side information is 600 bps. Its content can take the form of synchronization information, signaling bits, networking information, etc. It is not used in this first radio version, and random bits are transmitted instead.

3.4 Interleaver

An interleaver follows the multiplexer (Fig. 1), in order to spread in time the transmitted information. This is important in order to exploit the full potential of the channel decoding algorithm. The interleaving rule should be such that the received coded bits, on a branch of the code trellis and its neighboring branches, are not affected by the same fade on the mobile channel. Also, the coded bits on a branch of the trellis should be separated in time as much as possible.

The interleaver operation consists in grouping two 96-bit frames into a 192-bit superframe. The superframe bits, numbered from 1 to 192, are then shuffled with the help of the interleaver matrix shown in Fig. 3. The bits are output from the interleaver according to the occurrence of their respective number, when the matrix is read from the first line to the last and from left to right. In Fig. 3, the plain type numbers refer to the first frame bits (1 to 96), and the boldface numbers refer to the second one (93 to 192). The six rectangular boxes, as indicated in Fig. 4, refer to bits that are output from lines A to F in Fig. 2. This grouping is such that the two outputs from the $^2/_3$ coder (B and C) and the three outputs from the $^1/_3$ coder (D, E and F) are as distant as possible. This is assured by not having any of the blocks, pertaining to the same coder, overlap vertically with the other blocks of the same output.

1	2	3	4	5	6	7	8	9	10	11	12	13	14	15	16
97	**98**	**99**	**100**	**101**	**102**	**103**	**104**	**105**	**106**	**107**	**108**	**109**	**110**	**111**	**112**
17	18	19	20	21	22	23	24	25	26	27	28	29	30	31	32
113	**114**	**115**	**116**	**117**	**118**	**119**	**120**	**121**	**122**	**123**	**124**	**125**	**126**	**127**	**128**
33	34	35	36	**129**	**130**	**131**	**132**	62	65	68	71	63	66	69	72
37	39	40	42	43	45	46	48	**158**	**161**	**164**	**167**	**159**	**162**	**165**	**168**
133	**135**	**136**	**138**	**139**	**141**	**142**	**144**	74	77	80	83	75	78	81	84
49	51	52	54	55	57	58	60	**170**	**173**	**176**	**179**	**171**	**174**	**177**	**180**
145	**147**	**148**	**150**	**151**	**153**	**154**	**156**	86	89	92	95	87	90	93	96
61	64	67	70	73	76	79	82	**182**	**185**	**188**	**191**	**183**	**186**	**189**	**192**
157	**160**	**163**	**166**	**169**	**172**	**175**	**178**	38	41	44	47	50	53	56	59
85	88	91	94	**181**	**184**	**187**	**190**	**134**	**137**	**140**	**143**	**146**	**149**	**152**	**155**

Fig. 3: The interleaver matrix.

Examining the interleaver table, one notes that an error burst, which is not longer than 16 bits, does not affect the bits on the same or adjacent branches of the trellis. Also, the smallest distances between two bits are 4, 5 and 6 bits, and occur respectively between the pair of bits with position numbers (33,37), (34,39), (35,40) and (36,42). These small distances are not harmful since they occur between the *uncoded* block A and the *coded* block B. The next smallest distance is 12, and occurs either in block A, between pairs (117,129), (118,130), (119,131) and (120,132), or in block D, between pairs (169,181), (172,184), (175,187) and (178,190). The occurrence in block A is not much of a problem since these bits are not coded. The occurrence in block D means that double errors will be spread 12 branches apart after deinterleaving. The next possible distance is 53. This is large enough to assure independence between the coded bits, as required by the Viterbi algorithm.

It should be noted that this matrix arrangement is not necessarily optimum, and was obtained

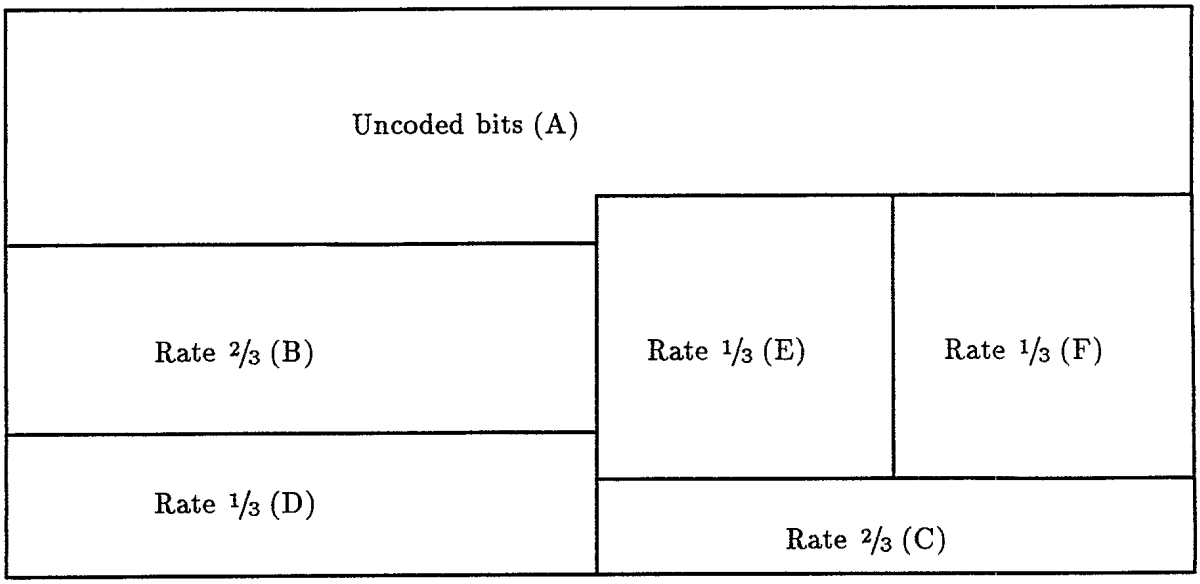

Fig. 4: The partitioning of the interleaver matrix.

by trial and error. Other arrangements which guarantee approximate statistical independence with a tolerable delay can be used. The grouping of two frames introduces a processing delay of two frames (40 msec) in the transmitter, and the corresponding deinterleaving adds another 40 msec delay in the receiver.

3.5 Bit Mapping

Following the interleaver (Fig. 1) is a mapping of the bit stream into a sequence of four-level symbols. The Grey coded assignment shown in Table 4 is used. This mapping allows differential detection in the receiver, where the real part is related to the first bit of the pair, and the imaginary part related to the second bit.

Bit pair	Symbol α
00	-3
01	+3
10	-1
11	+1

Table 4: The bit mapping table.

3.6 Preamble and Postamble

The preamble is a unique sequence of symbols, which is transmitted at the beginning of every message. It allows the receiver to detect the presence of a transmission, to correct the carrier frequency error between the two units, to synchronize the symbol timing and finally, to synchronize the 96-bit frame timing. In order to accomplish these tasks, the preamble is separated into three distinct types of symbols, as described in Table 5.

The symbols in section 1 of the preamble are used for detecting the presence of a communication and for computing the carrier frequency error between the transmitter and the receiver. These symbols are the samples of a pure DC tone (at baseband) and are transmitted without further processing. Symbol timing acquisition is computed using the alternating pattern of section 2 of the preamble, which is also transmitted without being CPM modulated. The final section is made of a CPM-modulated unique 126-bit PN sequence, which allows the determination of the beginning of the voice coded frames.

The postamble is made of the same unique 126-bit PN sequence used in the preamble. It allows the detection of the end of message. The signal processing performed by the receiver on these two special sequences is described in Section 4 of this report.

Preamble section	Duration	Type of baseband symbols	Modulation
1	126 symbols	1+j	none
2	106 symbols	-1+j, 1-j, -1+j, 1-j, ...	none
3	126 bits or 63 symbols	Grey coded 4-level	CPM
Total	295 symbols		

Table 5: The preamble symbol allocation.

3.7 CPM Modulation

Modulation, at the symbol rate of 2400 symbols/sec, is accomplished with the CPM format. The complex baseband representation of the modulated signal $s(t)$ is

$$s(t) = \exp\left[2\pi h \sum_{i=-\infty}^{i=\infty} \alpha_i q(t - iT)\right], \tag{2}$$

where h is the modulation index equal to $1/4$, α_i represents the sequence of symbols taken from the set $\pm 1, \pm 3$, T is the symbol duration and the phase pulse $q(t)$ is given by

$$q(t) = \int_{-\infty}^{t} g(\tau) d\tau, \tag{3}$$

where the frequency pulse shape $g(t)$ is such that its Fourier transform is

$$G(f) = \frac{N_1(f)}{T\text{sinc}(fT)}, \tag{4}$$

with $N_1(f)$ being the Fourier transform of the 20% raised cosine pulse. This choice of frequency pulse $g(t)$ gives a CPM signal which can be differentially detected without any inherent intersymbol interference. It is one of the modulation format retained for the Project 25. This modulation format allows the transmission of 4800 bps in a channel bandwidth of 6.25 kHz, with an adjacent channel rejection of more than 70 dB in the middle of the band. An example of the simulated power spectral density of the modulated signal is given in Fig. 5.

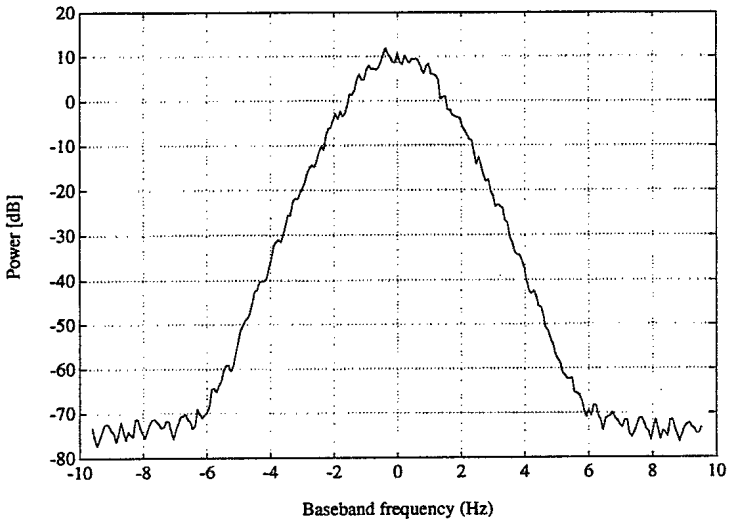

Fig. 5: The power spectral density of the modulated signal.

4 Receiver

The receiver block diagram is illustrated in Fig. 6. The received signal is filtered by the RX filter, whose function is to reduce to a minimum the interference imposed on the transmitted signal by the channel. This is done by filtering out a large part of the noise, outside of the signal bandwidth, and by removing some of the intersymbol interference introduced by the frequency conversion chains. The RX filter is therefore an equalizer, which is selected to make the radio performance optimum.

In idle conditions, the receiver continuously monitors the RX filter output, attempting to detect the presence of a message. If this presence is recorded, then a synchronization phase is entered, in which the initial carrier frequency error is computed, the initial symbol timing error is computed and corrected, and the beginning of a frame is determined. All of these functions are performed in

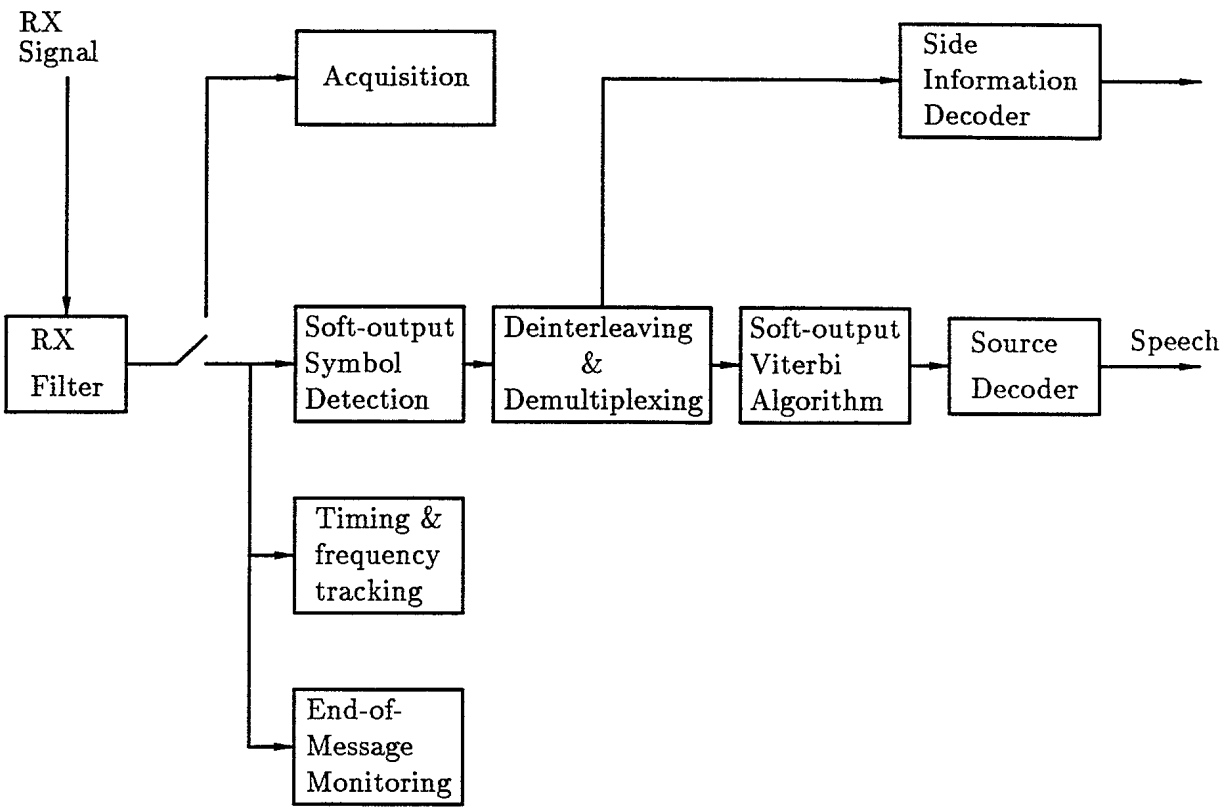

Fig. 6: Receiver block diagram.

the acquisition algorithm. Once the acquisition is declared, the tracking and detection part of the receiver takes over.

The tracking function allows the optimum symbol sampling time and carrier frequency deviation to be continuously monitored and updated. The receiver also searches for the end-of-message occurrence, by looking for the presence of the postamble sequence. These tracking and monitoring functions occur in parallel with the detection and decoding phase of the receiver.

4.1 The RX Filter

In this first implementation of a narrowband radio, the RX filter is fixed and is obtained by computing the Wiener filter corresponding to an AWGN channel, at Eb/No = 15 dB, for a known transmitted sequence of symbols. This filter therefore minimizes the effect of the channel inter-symbol interference and noise on the mean squared error (MSE) between the filter output and the known transmitted signal. It is optimum, in the MSE sense, only in these specific channel

conditions, but experience has shown that this kind of filter leads to very good performance for CPM signals on fading channels [7]. The choice of Eb/No = 15 dB is governed by the fact that differential detection gives a good bit error rate (BER) performance on an AWGN channel, as can be observed in Fig. 7. The figure also shows a slightly degraded performance when the RX filter is computed for a channel with Eb/No = 7 dB.

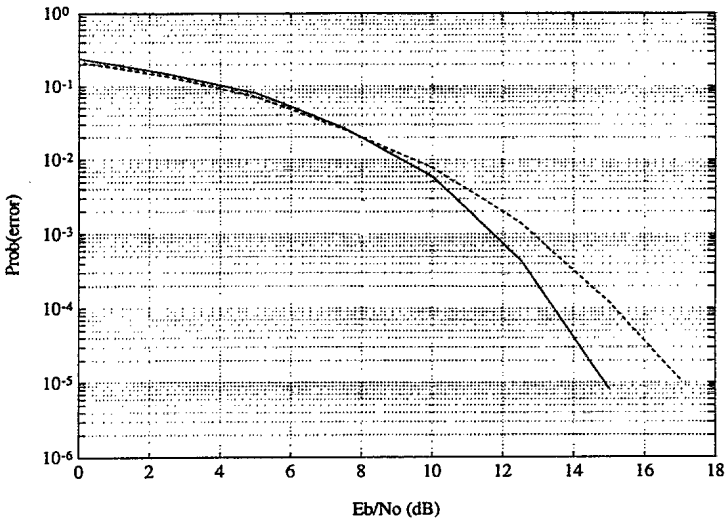

Fig. 7: The simulated bit error rate performance, for differential detection on an AWGN channel, with the RX filter given by a Wiener filter computed at Eb/No = 15 (plain curve) dB and at Eb/No = 7 dB (broken curve).

4.2 Acquisition

The acquisition procedure processes the preamble, previously described in Subsection 3.6 as consisting of a *pure DC section*, used for detecting the presence of a transmission and for computing the initial frequency error, an *alternating signal section*, used for estimating the initial symbol timing error, and a *pseudo-random section*, serving the purpose of finding the exact beginning of a frame. The processing of each of these sections is described in more detail below.

Detection of transmission

The presence of a message is determined with an algorithm of the form given in Fig. 8. This processing is designed in order to allow a decision on the presence of a known signal. The beginning of the preamble, for every message, is a pure DC component (at baseband) and the algorithm has to decide on the presence of such a signal, assuming a certain amount of additive white background noise. This is a radar problem, which is solved by first estimating the energy of the incoming signal, and by comparing it with the energy at a former time [8].

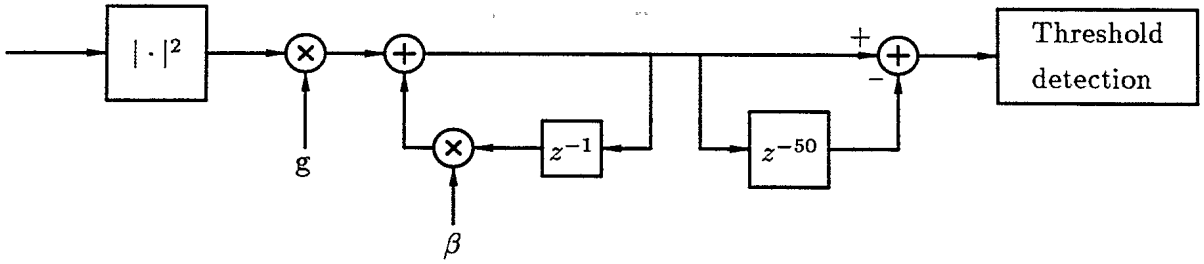

Fig. 8: The algorithm for determining the presence of a transmission.

The input signal is first processed by a square law detector. It is then scaled, essentially for adjusting the signal to the fixed-point precision of the processor, and averaged. The integration is performed by a one-pole infinite impulse response (IIR) filter, with the pole located at $\beta = 0.9$. The result is continuously compared with the integrated value computed 50 samples before. The delay of 50 is chosen because it represents approximately five times the time constant of the integrator, which is given by

$$\text{time constant} \approx \frac{1}{1-\beta} = 10. \tag{5}$$

The comparison is therefore between the energy at the present time, with the energy at a time taking the memory delay of the integrator into account. The performance of such a scheme can be estimated with the help of radar theory.

The signal-to-noise ratio after integration, denoted as $(\text{SNR})_i$, is given by [8]

$$(\text{SNR})_i \approx 10 \log L + \text{SNR} - 6 - 1, \tag{6}$$

where L is the memory of the integrator, SNR is the signal-to-noise ratio at the input, the factor of 6 dB is a worse case degradation, for $1 \leq L < 100$, due to the square law detector ([8], p. 31, Fig. 2.8-b), and the factor of 1 dB is the degradation due to the use of an integrator with a pole lower than one ([8], p. 391).

In order to have a *probability of detection* larger than 99%, the value of $(\text{SNR})_i$ must be around 16 dB ([8], p. 28, Fig. 2.7). This gives an *occurrence of false alarm* smaller than once per day ([8], p. 26, Fig. 2.5). With $L = 50$ and $(\text{SNR})_i = 16$ dB, the input SNR is then around 6 dB, which translates into

$$\frac{\text{Eb}}{\text{No}} = \text{SNR} \times \frac{\text{NBW}}{\text{R}} \approx 6 + 10 \log \left[\frac{6.25 \quad \text{kHz}}{4.8 \quad \text{kbps}} \right] \approx 7.15\text{dB}. \tag{7}$$

In (7), NBW and R refer respectively to the channel noise bandwidth and bit rate.

The above computations indicate that the algorithm of Fig. 8 gives, when used on an AWGN channel at or above Eb/No = 7 dB, a high probability of detection and a low occurrence of false alarm. These figures are altered in the presence of fading, as the test results have shown.

Estimation of the initial carrier frequency error

The second part of the acquisition computes the carrier frequency error, and issues a correction signal to the frequency conversion hardware. The algorithm performing this function is illustrated in Fig. 9. It uses the rest of the pure tone part of the preamble to compute two 256-point FFTs, one per segment of 40 input samples. The energies in the two FFTs are summed, and the location of the maximum amplitude point is taken as an estimate of the frequency error. The sampling rate at the input of the algorithm being 4.8 ksps, the frequency resolution is 18.75 Hz. Such an algorithm can be shown to give an estimate with an RMS frequency error not larger than 18.75 Hz, for Eb/No's larger than 5 dB [9].

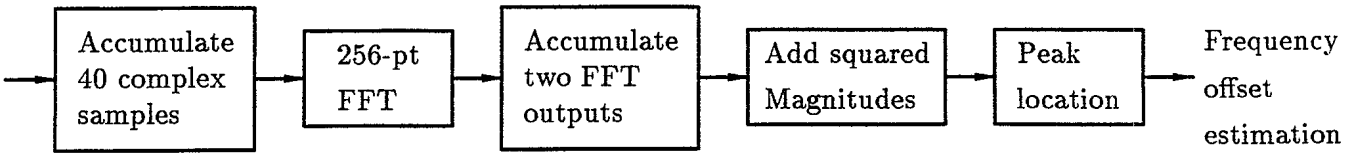

Fig. 9: The algorithm for computing the initial carrier frequency error.

Estimation of the initial symbol timing error

The third part of the acquisition computes and corrects the symbol timing error, as induced by the different time delays encountered during the transmission. The algorithm to perform this function is shown in Fig. 10. Although mainly based on *ad hoc* techniques, it has proven to be very effective in practice. As indicated in Subsection 3.6, the algorithm assumes an alternating transmitted sequence of complex symbols -1+j and 1-j, at a symbol rate equal to 2400 symbols per second. This sequence is therefore made of the samples of a complex sine wave at a frequency equal to 1200 Hz.

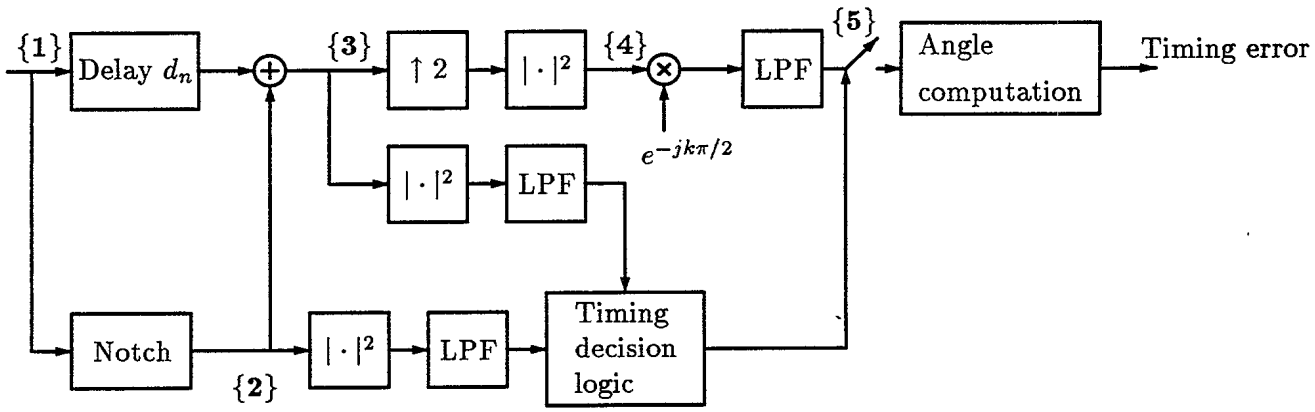

Fig. 10: The algorithm for computing the initial symbol timing error.

In the frequency domain, the received signal at point {1} in Fig. 10 is therefore represented

as two spectral lines at ±1200 Hz, imbedded in the channel noise [1]. The notch filter removes the two spectral lines and leaves intact most of the background noise. The energy of this noise signal is computed through the square law and lowpass filtering operations. The noise signal, at point {2}, is also subtracted from the delayed input signal, leaving at point {3} a filtered pair of spectral lines. The energy of this signal is computed and used, with that of the noise, in the *timing decision logic* algorithm to estimate the signal-to-noise ratio and to control the subsequent operations of the timing algorithm. At point {3}, the filtered complex sine wave is first interpolated by a factor of two and squared. This creates, at point {4}, a signal with a DC component and two spectral lines at ±2.4 kHz. Note that the interpolation operation is necessary since it is assumed that the input signal is sampled at 9.6 ksps. The signal is then down-converted with the complex exponential, such that the spectral line at +2.4 kHz is moved to 0 Hz. This DC component is isolated with the following lowpass filter. The result, at point {5}, is a phasor exhibiting an angle that is proportional to the timing error in the symbol sampling. When the *timing decision logic* has detected a proper signal-to-noise ratio, for a period of time equal to that of the processing delay of the top path of operations, the switch is closed and the phasor angle is computed. This timing error is used to skip the required number of samples and to adjust the interpolation delay at the front-end filter of the radio. This allows the output of the front-end filter to be sampled at instants that are very close to the optimum. The control of this sampling is then passed to the *symbol timing tracking* algorithm.

Estimation of the beginning of a frame

The last part of the preamble consists in a modulated 126-bit pseudo-random sequence. After the end of the symbol timing recovery, the received signal is sampled once per symbol and differentially detected. The resulting symbols are correlated with a local replica of the pseudo-random symbol sequence, and the start of the frame is determined in relation with the maximum of this correlation. The exact start is obtained when a significant increase in the correlation is recorded. This process ends the acquisition phase, and the receiver switches to the tracking and detection algorithms.

4.3 Timing and Frequency Tracking

The timing and frequency tracking functions allow respectively for the compensation of unknown delays imposed on the transmitted signal, and of the frequency deviations caused by the drifting in one or more oscillators.

Symbol timing tracking

The algorithm for tracking the optimum symbol sampling time is illustrated in Fig. 11. It is a closed-loop system, using a nonlinearity to generate some discrete spectral components from the modulated CPM signal [10]. The output of the front-end filter is first interpolated by two, in order to avoid aliasing later in the processing. A fourth-power nonlinearity is then applied on the 4-ary CPM signal. This generates a series of spectral lines at $\pm f_s/2$ and $\pm 3f_s/2$, where f_s is the symbol

[1] Unless otherwise noted, we assume an AWGN channel in this Subsection.

frequency. The bandpass filter (BPF) allows the removal of the noise and fading effects around these lines. The bandwidth of the passband regions must therefore be large enough to accommodate the frequency error induced by the channel fading. The squared magnitude operation, following the BPF, allows a constructive combination of the spectral lines at the symbol rate f_s, and a removal of a large part of the phase errors due to the fading process [10]. This strong component at the symbol rate is down-converted to 0 Hz and averaged through the lowpass filter. The angle of the resulting phasor gives the timing error that controls the sampling delay of the front-end filter. This filter is chosen from a bank of eight filters, each one being a version of the others, delayed by a multiple of $1/8$ of a *sample* duration. Since the front-end filter is operated at four times the *symbol* rate, the timing tracking operation then allows a tracking precision of $1/32$ of a symbol.

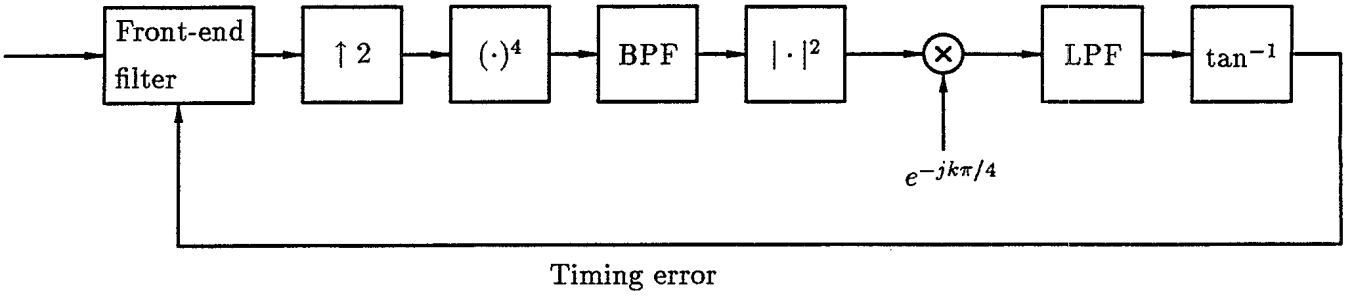

Fig. 11: The algorithm for tracking the optimum symbol timing instant.

Carrier frequency tracking

The frequency tracking function of the prototype radio has not been implemented at the time of the writing of this report. Assuming fairly stable oscillators and VCOs, this is not a critical function required for the narrowband radio trials. Based on past experience, it is believed that a simple method using a delay-and-multiply approach can be used with profit [11].

4.4 End-of-Message Monitoring

The radio is equipped with a function that continuously monitors, in parallel with the symbol tracking and detection, the signs of an end of transmission. A normal termination of message occurs when the receiver, through a correlator-type of processing, detects the presence of the unique postamble sequence. When this is accomplished, the radio returns in idle operation, waiting for the presence of a new transmission.

The radio also performs a check for an abnormal loss of message. This may happen when the message ends and the postamble is not detected, due to extreme channel conditions. A mean to detect this situation is necessary, in order to avoid the voice decoder to output noisy unwanted sounds. The radio therefore monitors the energy in the incoming signal. If this energy drops significantly for a long enough time, loss of signal is declared. This processing is similar to that of

the first part of the acquisition, illustrated in Fig. 8, except for the monitoring of a drop in energy, instead of an increase.

4.5 Symbol Detection and Bit Recovery

The symbol detection and bit recovery sections of the receiver are labelled in Fig. 6 as *soft-output symbol detection*, *deinterleaving and demultiplexing*, *soft-output Viterbi algorithm* and *Source decoder*. These functions are treated in the following subsections.

4.5.1 Soft-Output Symbol Detection

The symbol detector delivers soft outputs, in order to allow the subsequent signal processing algorithms to perform optimally. Soft-output decisions are such that some information is available about the reliability of every decisions. This type of signal is obtained directly from a differential detector, if the bit to CPM symbol assignment is done according to Table 4. The differential detector output $\hat{d}_n$ is such that the bit soft decisions are given by

$$\begin{aligned} \hat{b}_{n1} &= \mathrm{Re}[\hat{d}_n] \\ \hat{b}_{n2} &= \mathrm{Im}[\hat{d}_n]. \end{aligned} \tag{8}$$

This form of detection is far from being optimum in fading conditions. It has been implemented in the first prototype version because of its simplicity, and because it delivers soft-outputs, without carrier phase recovery, at a very low implementation cost. A much better method would be based on maximum likelihood sequence estimation (MLSE), which has been studied in [12] for flat-fading channels. The advantage of MLSE is that it does not produce a high irreducible error rate and does not require carrier phase recovery. Its main drawback is its complexity for a four-level modulation format, since it encompasses a dynamic programming algorithm (Viterbi algorithm). The complexity of the MLSE algorithm is proportional to q^M, with q being the number of symbols and M representing the decoding memory [12]. In addition, the generation of soft-output decisions with a Viterbi algorithm (VA) operating on a non-binary alphabet exhibits a high degree of complexity [13].

Nevertheless, a simplified form of this method would be of great interest, and further investigations into its implementation are described in Subsection 5.2.

4.5.2 Deinterleaving and Demultiplexing

The deinterleaving algorithm essentially reverts the shuffling imposed on the transmitted bits through the matrix of Fig. 3. The resulting voiced-related soft-decisions are rearranged in channel coded frames, while the side information decisions are sent to the proper decoder. The frames of RCPC soft-decisions are then sent to the channel decoder.

4.5.3 Soft-Output Viterbi Algorithm

For optimum source decoding, it is desirable for the channel decoder to output binary soft decisions. With such a binary symbol x, the decision reliability $L(x)$ is usually defined as the log-likelihood of this decision, i.e. [13]

$$L(x) = \log\left[\frac{\text{Prob}(x=1)}{\text{Prob}(x=-1)}\right]. \tag{9}$$

Each voice-related frame is decoded according to the RCPC allocation performed in the transmitter. This decoding is done by a Viterbi algorithm which produces soft-decision outputs. This soft-output Viterbi algorithm (SOVA) has been proposed in different formats [13], [14] and [15]. Basically, the conventional SOVA keeps track of the surviving paths and their associated likelihood differences along the code trellis. A trellis example is given in Fig. 12. In this example, the Viterbi algorithm has selected, at time j, the maximum-likelihood (ML) path as being the one in bold, with an accumulated metric equal to M_j^0. The magnitude of the accumulated metric difference at this point is labelled Δ_j^0. The differences, along the ML path are labelled as Δ_j^ℓ, for the time instant $j-\ell$. At instant $j-i$, the bit associated to a branch of the path discarded from the ML path at time $j-\ell$ is labelled x_{j-i}^ℓ.

The conventional SOVA updates the likelihood differences along the ML path with the following approximate formula [16]

$$\Delta_j^\delta \approx \min_{\ell=0,\ldots,\delta} \Delta_j^\ell, \tag{10}$$

where the minimum is taken only if $x_{j-\delta} \neq x_{j-\delta}^\ell$. An equivalent formula is

$$\Delta_j^\ell = \min(\Delta_j^\ell, \Delta_j^0) \qquad \ell = 0,\ldots,\delta, \tag{11}$$

where the minimum is again taken if $x_{j-\delta} \neq x_{j-\delta}^\ell$. The surviving likelihood differences are therefore updated for each new symbol, and their sign constitutes the conventional VA decision, while their magnitude represents the reliability information $L(x)$ concerning the surviving binary symbols. The SOVA requires therefore more memory to store the finely quantized magnitudes, in addition to the conventional memory required to store the path symbol decisions. It also necessitates more computations than the VA, since the reliability values are refined with each new input.

The SOVA implemented in the prototype radio is closely related to the channel coded frame structure. Because the transmitter inserts 4 *zero* bits at the end of each frame (see the end of Subsection 3.2), the channel decoder operates on a block basis. Each block has 60 bits, i.e. 24 2/3 coded bits, 24 1/3 coded bits and 12 end bits (corresponding to the 4 zero bits). The accumulated metrics are all set to zero at the start of the block decoding, and they are updated according to the formula

$$\begin{aligned} M_0^m &= 0 \\ M_j^m &= M_{j-1}^m + \sum_{i=1}^{3} \tilde{g}_{ij} a_{ij} x_{ij} y_{ij} \quad m = 0,\ldots,15 \quad j = 1,\ldots,60, \end{aligned} \tag{12}$$

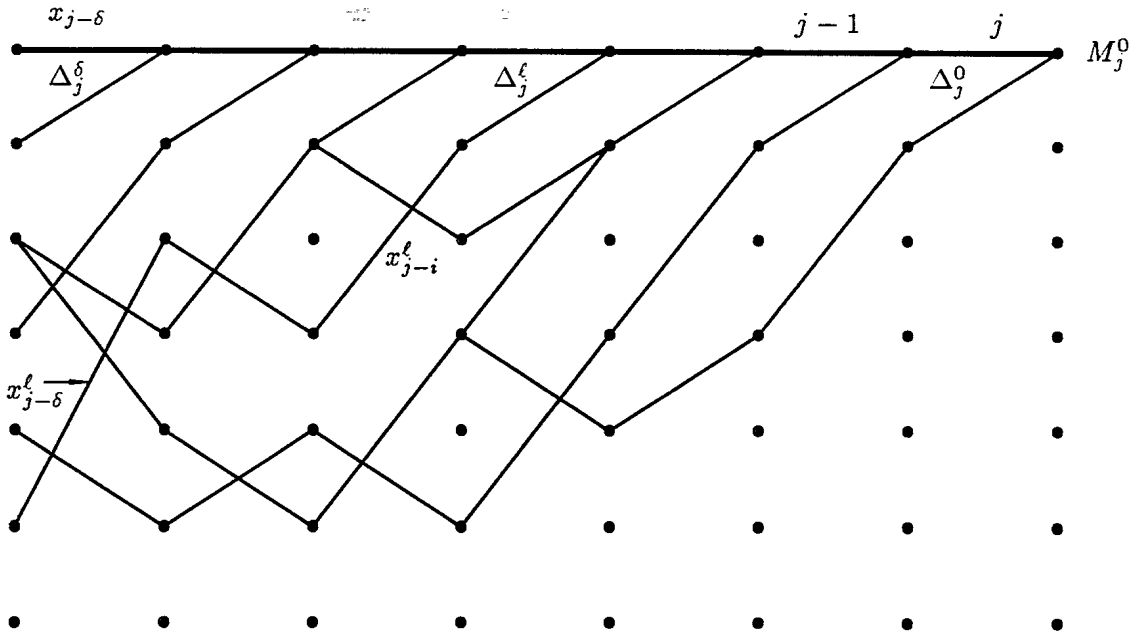

Fig. 12: A trellis example with some metric differences used in the derivation of the SOVA.

where x_{ij} is the i^{th} transmitted bit in the j^{th} branch, y_{ij} is the corresponding received soft-output from the symbol detector, $\tilde{g}_{ij}$ is the estimated channel gain for this time, and a_{ij} is the *puncturing flag*, equal to one if the bit was actually transmitted, and equal to zero otherwise.

The channel gain $\tilde{g}_{ij}$, also defined as the *channel state information*, is estimated as

$$\tilde{g}_{ij} \approx \sqrt{|\hat{d}_n||\hat{d}_{n-1}|}, \tag{13}$$

where $|\hat{d}_n|$ is the magnitude of the received channel symbol corresponding to the soft-output y_{ij}. The correspondence is made through the differential detector output rule, given in (8).

Once all the accumulated metrics of (12) are computed for the block, the ML path is selected as the survivor ending in state zero (since it is known in advance that the encoder outputs a string of zeros). At this stage of the radio development, the soft-output updates of (10) or (11) are not implemented, due to an erratic behavior in the updated values. This phenomenon is believed to be related to the multi-rate nature of the code. The soft-outputs are therefore taken to be the straight accumulated metrics, and are sent to the source decoder for further processing.

4.5.4 Source Decoding

The source decoder accepts the channel decoder soft-outputs and produces an estimate of the transmitted voice signal. The availability of the reliability of each bit decision allows the voice decoder to perform error concealment, by combining these SOVA outputs with the decisions and the reliabilities of the previous frames.

The efficient usage of the reliability information is still under investigation, but it is believed that many of the annoying sounds produced by the source decoder, when bit errors are encountered, can be substantially softened by repeating the bits of the previous frame, when a low reliability for these bits is computed.

The source decoding itself is the reverse process of the frame frequency analysis performed in the transmitter. The information contained in each frame, as shown in Table 1, is used in an inverse Fourier transform to regenerate the voice information.

5 Advances and Research Areas

The narrowband radio design, as discussed in the first part of this report, has been implemented and partially tested. Although its performance is very good in this first version, some improvements are still possible, through the use of even more sophisticated signal processing techniques. Three of these possible improvements are described in the following subsections, and constitute areas of research that could be pursued in a second phase of the radio development. These techniques are: *adaptive RX filtering*, *soft-output maximum likelihood sequence estimation*, and the *use of a priori information* in the channel decoder.

5.1 Adaptive RX Filter

The simulations and tests results have shown that a RX filter, designed as a Wiener filter, allows very good performance. An adaptive RX filter, based on the minimum mean square error (MMSE) criterion, therefore seems a good choice for the RX filter. Such a filter would trade off noise rejection with intersymbol interference cancellation, and would allow for the choice of relatively inexpensive filters in the frequency down-conversion hardware.

Since MMSE adaptive filtering performs poorly in the presence of fast fading conditions, a new adaptive equalization technique for CPM signals has been developed [17], [18]. This equalization method does not require carrier phase recovery and can therefore be used on fast fading channels. It also has the particularity that some of its intermediate computations can be used to generate channel state information. Its operation is based on the signal processing shown in Fig. 13.

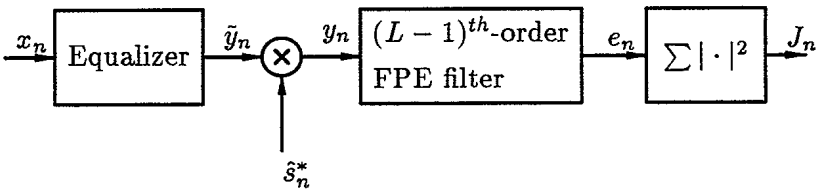

Fig. 13: A block diagram for the computation of the cost function J_n in the equalizer.

In this algorithm, the sampled received signal x_n is first linearly equalized by an FIR filter. The filter output is multiplied by the complex conjugate of either the estimated transmitted signal (obtained from the symbol detection decisions), or of a known training sequence. If the training

sequence is available at the receiver, or if the error rate is not high (typically under 10%), the result y_n is a combination of the fading process, the channel noise, and the intersymbol interference (ISI). This signal is filtered by an adaptive forward prediction error (FPE) filter, or by a highpass filter, which essentially produces an estimate of the channel noise and ISI. In the equalizer adaptation process, the energy J_n of this interference estimate is computed. The energy at the output of the equalizer is also computed and the equalizer weight vector is obtained by maximizing the ratio of these two values. This process is therefore an optimization, with respect to the equalizer weight vector, of a form of signal-to-interference ratio at the equalizer output. Since this optimization is not a function of the channel phase variations, there is no need to estimate the received carrier phase, which makes this equalization algorithm very effective, even in fast fading conditions [18]. On an AWGN channel, this method has also been shown to yield an equalizer that is completely equivalent to a MMSE filter [19].

A collection of adaptive algorithms for implementing the new form of equalizer has been proposed in [20]. The whole algorithm has a complexity proportional to M^3, where M is the number of coefficients in the equalizer. This is considered too prohibitive to be implemented in real time. A block-adaptive version has been instead considered [21]. This more realistic method is being studied extensively, with respect to fixed point finite word length problems, and will be implemented in the radio as an equalizer that is computed once per transmission, using the last part of the preamble (the pseudo-random section). This work is near completion, and the results will be documented soon.

5.2 Maximum Likelihood Sequence Estimation

It was shown in [12] that, for the special case of Rayleigh flat-fading and continuous phase modulation signaling, maximum likelihood sequence estimation could be implemented as a *linear predictive receiver*. This type of receiver is in the form of the Viterbi algorithm with the trellis updates being computed using a bank of FIR filters and square operations. This detector was shown to be very effective in fast fading conditions, in the sense that its performance exhibits either a very low irreducible error rate in the case of an approximately bandlimited fading power spectral density, or an arbitrarily small irreducible error rate in the strictly bandlimited case [12].

The superiority of the linear predictive receiver over simple detection schemes, such as differential detection, is obtained at the expense of computational complexity and memory requirements. In particular, if the combined channel fading and noise can be estimated by an Lth order autoregressive process, then the linear predictive receiver consists in a bank of $rq^{\lceil \alpha+\beta \rceil}$ filters[2] and a Viterbi algorithm with $q^{\lceil \alpha+\beta \rceil - 1}$ states. The parameter r represents the number of samples per symbol used in the receiver, q is the size of the symbol alphabet, α is the length, in symbols, of the CPM frequency pulse, and $\beta = L/r$.

For a *quaternary* CPM scheme ($q = 4$), assuming that a minimum of two samples per symbol are necessary to avoid too much aliasing, that the CPM frequency pulse can be approximated by only three symbol periods ($\alpha = 3$), and that a 5th-order predictor ($L = 5$ and $\beta = 2.5$) is sufficient,

[2]The notation $\lceil a \rceil$ represents the smallest integer greater than or equal to a.

the receiver requires 8192 filters and a trellis of 1024 states, with 4096 branch updates. This is clearly too complicated to be implemented.

The requirements for soft-outputs from the MLSE algorithm also add to this complexity. An important area of research is therefore related to the problems of complexity reduction and soft outputs computations. Two methods for reducing the computing requirements are currently under investigation [22]. In the first one, the number of states is reduced by approximating the frequency pulse and the linear prediction of the fading plus noise process with smaller lengths impulse responses. The second method is based on the M algorithm, which retains, at a given trellis level, only M paths for extension to the next level [23]. This M algorithm is coupled with a modified version of the q-ary Soft Output Viterbi Algorithm (QSOVA) of Li *et al.* [24]. The QSOVA is based on the accumulation of MLSE metrics, for each trellis state, given that a certain symbol was transmitted in a certain time slot in the past. The minimization of the accumulated metrics, for each of the symbols, delivers unquantized values that can be directly used as soft outputs.

The final results of this research could lead to the implementation of a simplified, yet effective, MLSE algorithm in the narrowband radio.

5.3 Use of *a priori* Information in the Viterbi Algorithm

The use of a multi-rate channel code for protecting more heavily some of the source parameters, as described in Section 3.2, is one way of combining source and channel coding and decoding methods. Another form of such combined decoding takes advantage of two sources of information traditionally overlooked: the signal correlation left at the source encoder output and the availability of some reliability information, as produced by the SOVA. A high bit correlation means that certain bits change infrequently. The decoder may therefore acquire knowledge, with a certain probability, of these bits by extrapolating the information in the previous bits. One method, for the Viterbi algorithm, to make use of the residual correlation left in the source bits is to incorporate *a priori* information in the metric computations [16]. This soft-output Viterbi algorithm with *a priori* information (APRI-SOVA), is a modified version of the SOVA in which the metric update of (12), is done according to

$$M_j^m = M_{j-1}^m + \sum_{i=1}^{3} \tilde{g}_{ij} a_{ij} x_{ij}^m y_{ij} + x_{ij} \cdot L(x_{ij}) \quad m = 0, \ldots, 15 \quad j = 1, \ldots, 60, \tag{14}$$

where $L(\cdot)$ is the reliability function of (9). Then, by assuming that the frame-to-frame correlation among the source bits follows a first-order Markov model, the value of $L(x_{ij})$ can be obtained from a combination of the previous SOVA output $L(\hat{x}_{ij})$, with an estimate of the probability P_{tn} that this particular bit experiences a change [16]. This could be expressed as

$$L(x_{ij}) = L[\hat{x}_{ij} \oplus c_n], \tag{15}$$

where $\oplus$ is the modulo-two addition and c_n is the change bit with a probability P_{tn} of being equal to one.

For poor transmission links, such as those encountered frequently in a mobile environment, it has been shown [16] that error propagation is greatly reduced by the APRI-SOVA algorithm and that

the output speech quality is significantly enhanced. This method is actually under investigation in the radio development. The use of *a priori* information will be limited to the eight most sensitive source output bits, which have been described in Section 3.2 to be respectively the four most significant bits of the frame energy and of the frame fundamental frequency. Since it is observed that neither of these parameters change rapidly over time, a definite correlation between frames exists among these bits. The value of the change bit in (15) can therefore be estimated reliably from the overall value of the energy or frequency parameter, and used as described above.

6 Performance Tests

The ultimate test for a radio dedicated to voice transmission is the actual evaluation by the targeted group of users. Before this can be done efficiently and systematically, a series of laboratory tests was performed in order to characterize some of the radio functions. This set of tests can be summarized as follows:

- Measurement of the transmitted power spectral density.
- Probability of acquiring a transmission for different channel conditions.
- Error on the initial estimation of the frequency deviation.
- Probability of detecting the exact beginning of a coded voice frame.
- Bit error rates for different configurations of the timing tracking algorithm.

This series of tests is not exhaustive, but gives good indications of the radio performance. More elaborate tests would require some significant software modifications, and are being planned for a subsequent development phase. In particular, the performance of the initial timing acquisition algorithm has not been measured because of a lack of time.

The different channel characteristics were obtained by interfacing the transmitter and the receiver with a hardware channel simulator, operating at the intermediate frequency of 70 MHz.

6.1 Measured Power Spectral Density

The measured PSD is shown in Fig. 14. It is observed at the radio low IF, i.e. it is centered on 4.8 kHz. This figure should be compared to the simulated PSD of Fig. 5. It is noticed that the low IF forces some distortion in the 0–2 kHz range, and that some energy exists at more than 70 dB below the adjacent channel average power. This interference is probably due to some of the approximations used in the modulator implementation (see [1]).

The center frequency of 4.8 kHz was selected because it represents exactly one quarter of the radio sampling frequency (19.2 ksps), which leads to significant simplifications in the software implementation. A more precise procedure would be to output the transmitted signal at complex baseband, and to up-convert it in hardware. This would introduce more hardware, but would not be a major limitation and should be considered in a more sophisticated implementation.

6.2 Acquisition of a Transmission

The probability of acquiring a transmission versus Eb/N_o, and for different fading rates, is presented in Fig. 15. Recall from Subsection 4.2 that the algorithm for detecting the presence of a message, shown in Fig. 8, was designed to give a theoretical probability of detection larger than 99%, for Eb/No superior to 7 dB and no fading. The corresponding measured performance is very close to the theory. When the fading rate is increased to nonzero values, the average performance tends to become better, except for a fading rate of 25 Hz. The better performance in fading conditions can be explained by the random channel gain, which modifies the energy of the received signal, thereby creating more energy variations susceptible to trigger signal detection. Note that false alarms were not experienced within any period of normal use.

6.3 Error on the Initial Estimation of the Frequency Deviation

The standard deviation on the estimate of the initial frequency error is illustrated in Fig. 16, for three values of fading rate. The frequency error was computed only when the receiver had been able to detect the presence of a message. It is noticed that below a certain threshold, the variance of the error becomes large, and the computations are not very reliable. Above this threshold, the error variation is stable and increases with the fading rate. The threshold itself decreases with the fading rate, which is a consequence of the spreading in energy induced by the fading process. Although not shown here, it was noticed that on a channel without fading, the frequency error deviation was essentially always zero, for Eb/No's large enough to allow a reliable message detection.

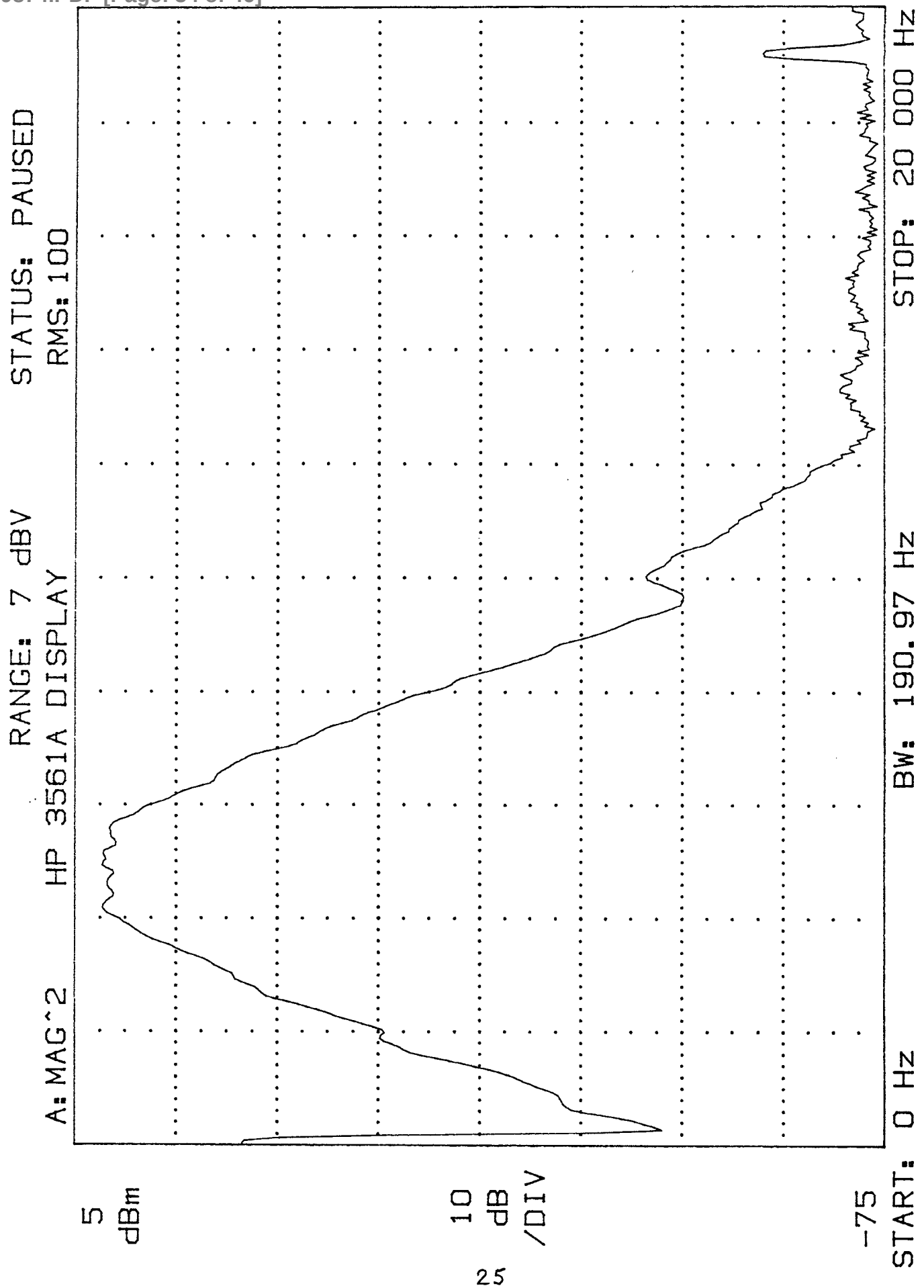

Fig. 14: The measured power spectral density at the modulator output.

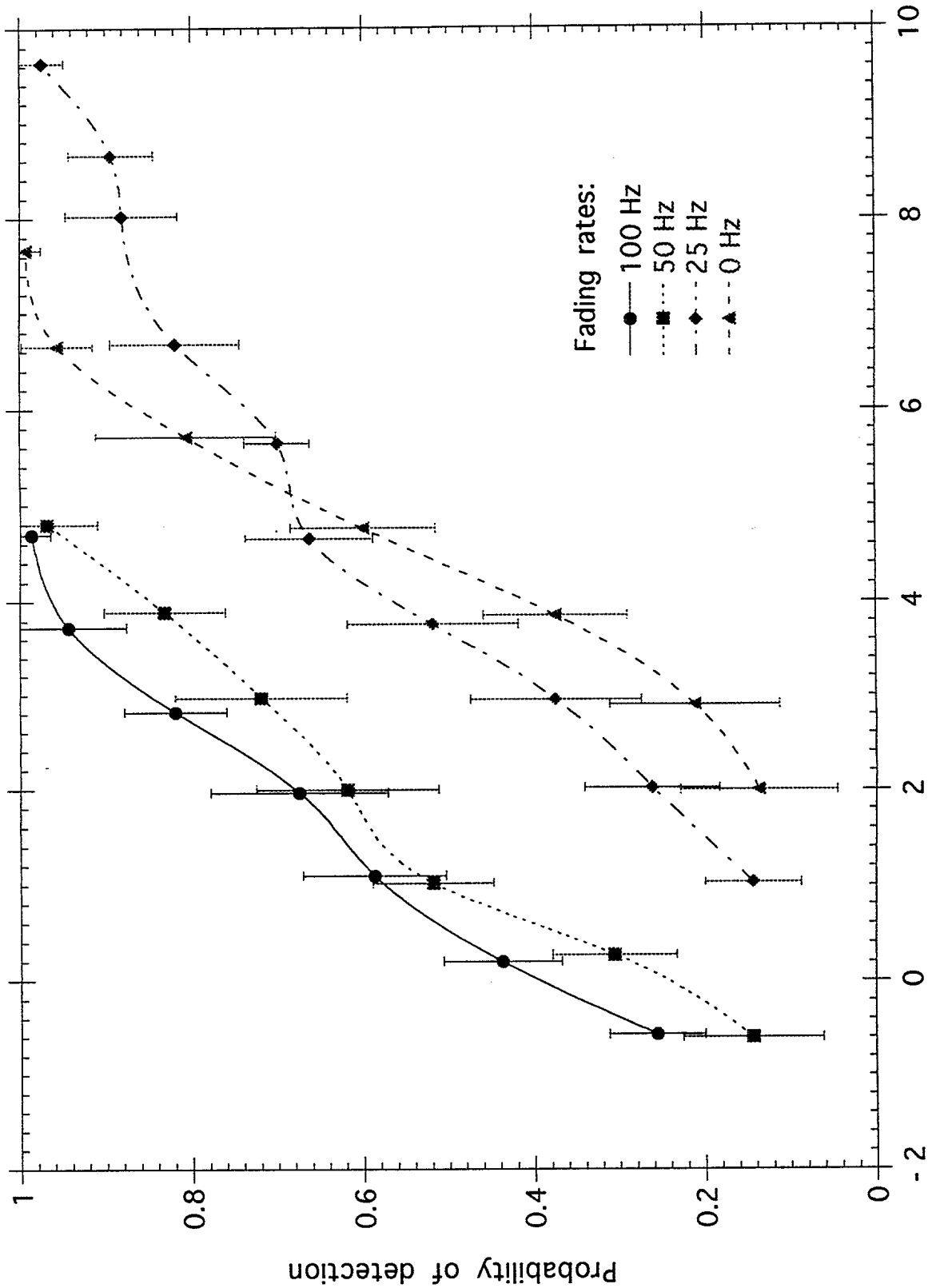

Fig. 15: The probability of detecting the presence of a message on a Rayleigh fading channel.

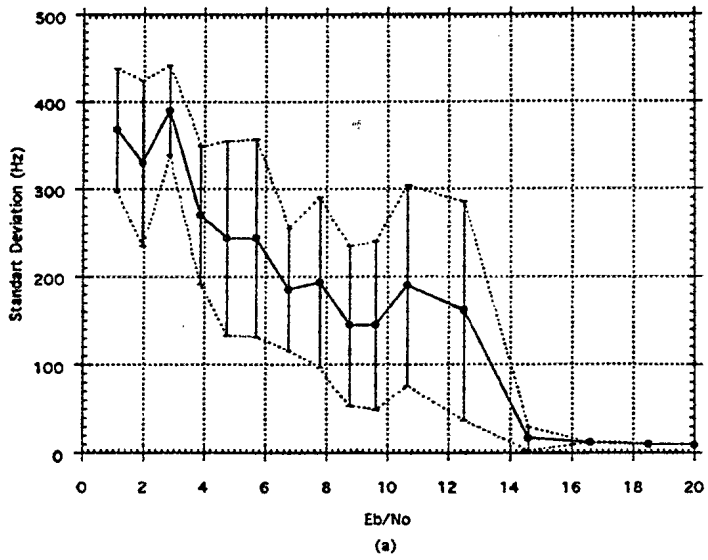

(a)

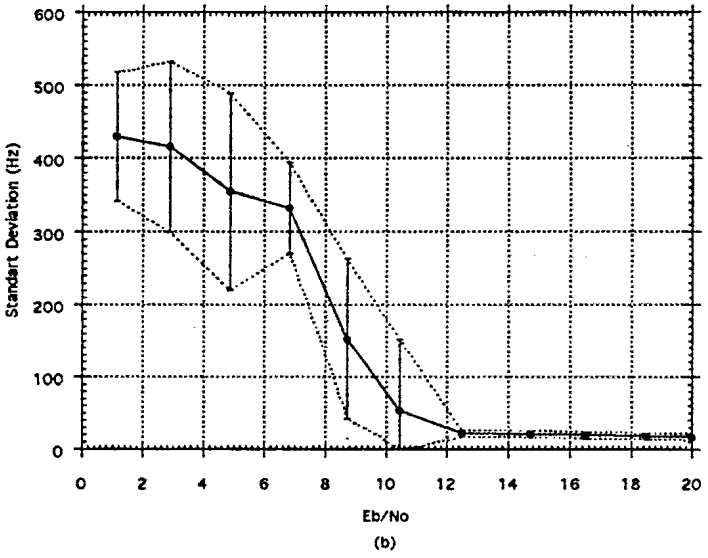

(b)

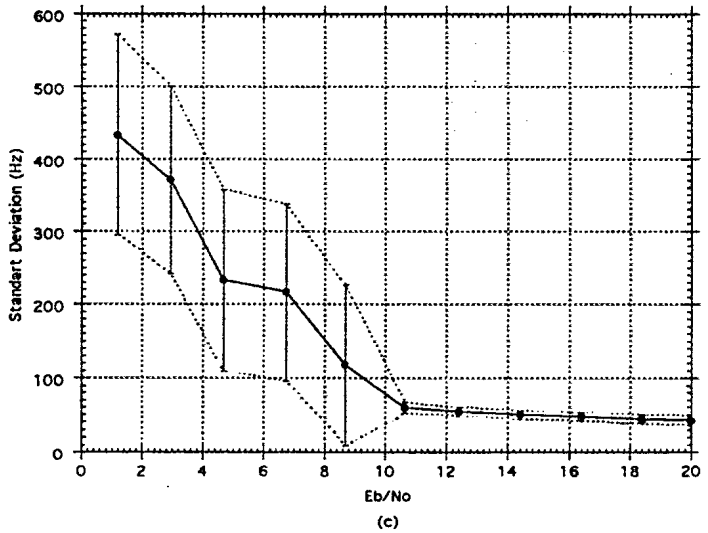

(c)

Fig.16: The standard deviation on the estimate of the initial carrier frequency error on a Rayleigh fading channel; fading rate = (a)25 Hz, (b)50 Hz, (c)100 Hz.

6.4 Probability of Detecting the Exact Beginning of a Coded Voice Frame

The probability of correctly estimating the location of the preamble unique word is shown in Fig. 17, for two fading rates. This probability was measured only when the radio had successfully detected the presence of a message, and estimated adequately the initial timing error. In AWGN conditions, the exact frame beginning was almost always detected, and no meaningful statistics were collected in this case. For fading rates of 25 and 50 Hz, the probability is larger than 80%, when Eb/No is over 8 dB. The tests of this section, along with those of the two previous ones, show that the receiver is very likely to acquire correctly a transmission, as long as Eb/No is larger than 10 dB.

6.5 Measured Bit Error Rates

In order to assess the radio performance, in term of data transmission, three series of BER tests were performed. In all of these tests, perfect acquisition by the receiver was accomplished and no channel coding was used. The transmitter and the receiver were first operated from the same master clock, and the timing tracking was disabled. The results of this first series of tests are shown in Fig. 18 [3], along with the simulated curve of Fig. 7. In the case without fading, the difference between the simulated and the measured curves is the result of the intersymbol interference introduced by the up and down conversion hardware. This equipment is used to interface the radio and the channel simulator. Most of this degradation should disappear when the adaptive RX filter described in Subsection 5.1 is implemented. As for the cases with Rayleigh fading, the performance curves are grouped for fading rates ranging from 1% of the symbol rate (25 Hz) to 4% of the symbol rate (100 Hz). Since the vocoder starts to show a noticeable degradation for BER higher than 1%, the radio performance, without channel coding, would become less reliable at Eb/No lower than 20 dB.

The very small degradation introduced by the jitter in the symbol timing algorithm can be appreciated by inspecting the curves of Fig. 19, and by comparing them with those of Fig. 18.

Finally, the BER performance with two completely independent units are presented in Fig. 20. The performance without fading is very close to the one of the preceding figures. When fading is present, the symbol tracking algorithm is less effective at following the clock differences, and the performance is degraded.

It appears, from these results, that some more fine tuning of the symbol timing tracking algorithm is necessary. On the other hand, the listening tests described in the next subsection show that a reliable voice communication is possible under these fading conditions, provided that channel coding is used.

[3] All the BER measurements presented in this subsection were obtained by gathering enough statistics to produce negligible or very small measurement uncertainty.

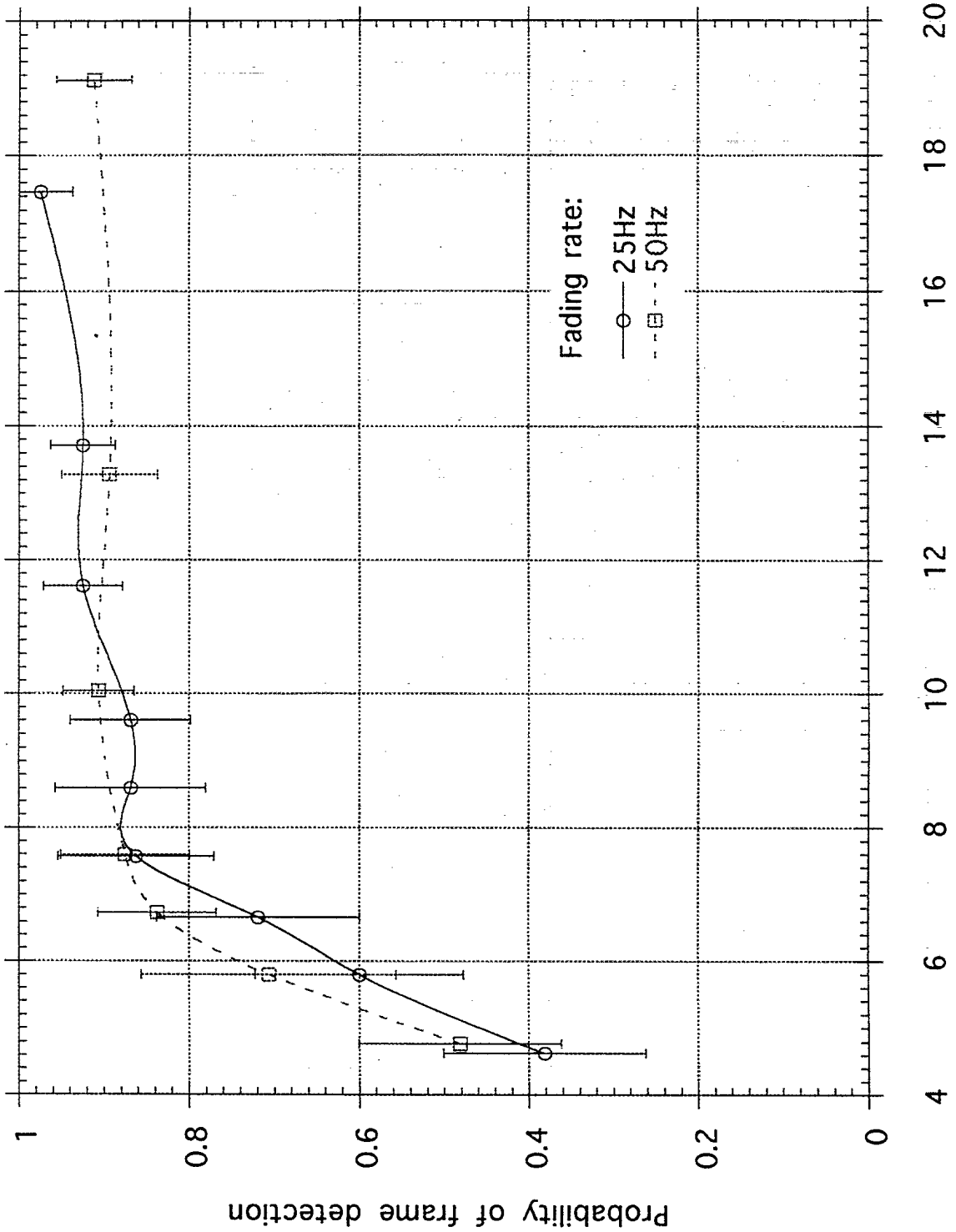

Fig. 17: The probability of detecting the beginning of a frame on a Rayleigh fading channel.

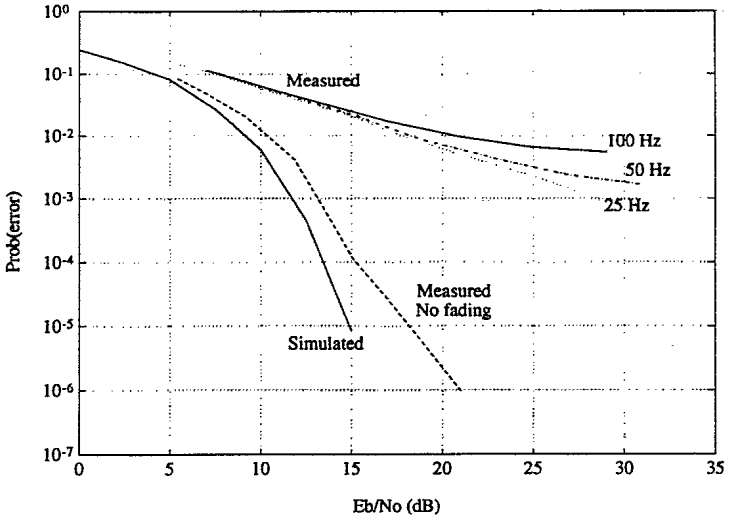

Fig. 18: The measured bit error rate performance, for *identical* radio sampling clocks and *no* timing tracking. *No channel coding included.*

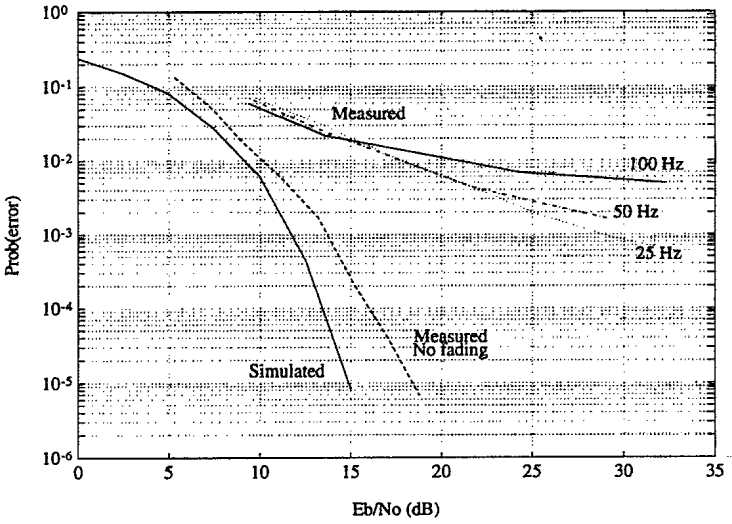

Fig. 19: The measured bit error rate performance, for *identical* radio sampling clocks and timing tracking. *No channel coding included.*

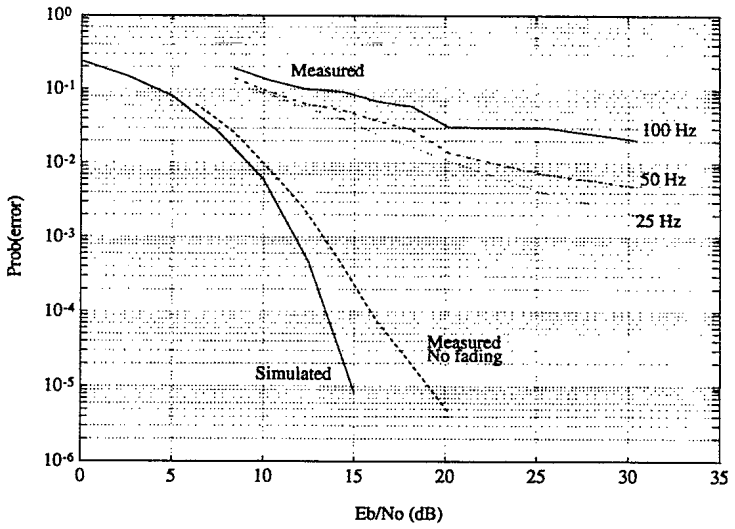

Fig. 20: The measured bit error rate performance, for *different* radio sampling clocks and timing tracking. *No channel coding included.*

6.6 Performance with Channel Coding

The BER results of the previous subsection have shown that an Eb/No larger than 20 dB would be required for adequate voice transmission, if no channel coding is used. The tests of Subsections 6.2 to 6.4 indicate that the radio is very likely to acquire a communication, and to synchronize itself, for Eb/No's larger than 10 dB, with Rayleigh fading rates up to 4% the symbol rate.

It then appears that channel coding is indeed necessary to give good voice communication at Eb/No's lower than 20 dB. The performance of the channel coding, described in Subsection 3.2, and of the corresponding decoding, treated in Subsection 4.5, has been evaluated by informal listening tests in various channel conditions. The transmitter and the receiver were two independent units, each one using its own local clock. The channel conditions that were considered are listed in Table 6. A recorded tape is available, with voice segments of one minute duration for each channel state.

The channel conditions indicated in the table represent extreme values, in term of voice quality. In the case of no fading, the voice quality is fairly good for Eb/No=10 db[4]. At Eb/No=5 dB, the voice quality is fairly degraded. This is also the case for Eb/No=13 dB and a fading rate of 100 Hz, and for any Eb/No at a fading rate of 200 Hz. At a higher fading rate, the voice quality becomes very bad, indicating that some of the receiver algorithms do not perform well in these extreme conditions.

These listening tests show that usable voice communication is possible, although not of very

[4]Note that the value of Eb/No used with channel coding is that of the *channel bits*, at a rate of 4800 bps, as opposed to that of the source bits alone. The value of C/No is given by adding 10 log(4800)=36.8 dB to the value of Eb/No.

Eb/No (dB) (channel bits)	C/No (dB-Hz)	Fading rate (Hz)	Voice quality
∞	∞	0	very good
10	46.8	0	good
8	44.8	0	fair
5	41.8	0	poor
20	56.8	100	fair
13	49.8	100	poor
∞	∞	200	poor
20	56.8	200	poor

Table 6: The channel conditions used for the listening tests.

good quality, at C/No = 42 dB-Hz on an AWGN channel. The same is true at fading rates up to 8% the symbol rate (200 Hz), when C/No is larger than 55 dB-Hz. It is interesting to note that a radio using a conventional narrowband frequency modulation approach, in a 25–30 kHz channel bandwidth, requires a C/No over 50 dB-Hz on an AWGN channel, and over 60 dB-Hz on a moderately severe fading channel, in order to give the same voice quality [11]. This indicates that the radio implementation described in this report is very robust in fairly severe channel conditions.

7 Conclusion

The fundamental building blocks of an implementation of a narrowband mobile radio, using state-of-the-art signal processing algorithms, have been presented. The techniques used in the implementation include combined source and channel coding, efficient adaptive equalization on fading channels, soft-output symbol detection, and combined channel and source coding/decoding. The relationship between the different algorithms has been described. These methods, although computationally extensive, have lead to a very effective narrowband mobile radio transmission scheme. A radio prototype has been built and tested in real time, under laboratory conditions. This first prototype version requires more testing and evaluation, and some important research areas are still left for investigation. It is believed that this radio is one of the most advanced of its kind, and that it is the precursor of the future generations of mobile radios.

References

[1] Y. Jolly, P. Benoit, D. Boudreau, *The implementation of a narrowband radio for tactical and civilian communications,* Communications Research Centre, Industry Canada, May 1995.

[2] APCO Project 25, *Common Air Interface*, Copyright MOTOROLA, INC, December 9, 1992.

[3] J. C. Hardwick and J. S. Lim, "A 4800 bps improved multi-band excitation speech coder," *Proc. of IEEE Workshop on Speech Coding for Tele.*, Vancouver, BC, September 1989.

[4] H. Hassanein, A. Brind'Amour, S. Déry and K. Bryden, "Frequency selective harmonic coding at 2400 bps," *Proc. of the 37th Midwest Symposium on circuits and Systems*, Lafayette, Louisiana, pp. 1436–1439, August 1994.

[5] H. Hassanein, A. Brind'Amour, S. Déry and K. Bryden, "Frequency Selective Harmonic Coding at 2400 bits per second (U)," *CRC Report, Industry Canada*, No. 94-001, version 1.3, Ottawa, November 1994.

[6] J. Hagenauer, "Rate-compatible punctured convolutional codes (RCPC codes) and their applications," *IEEE Trans. on Communications*, vol. 36, no.4, pp. 389–400, April 1988.

[7] D. Boudreau, *The Application of Feedback Decoding in the Differential Detection of Continuous Phase Modulated Signals*, M.Eng. Thesis, Faculty of Engineering, Carleton University, April 1987.

[8] M. I. Skolnik, *Introduction to Radar Systems, 2nd Edition*, McGraw-Hill, 1980.

[9] S. N. Crozier, "Performance and complexity comparison of discrete-time frequency estimation algorithms," *Proc. 17th Biennial Symposium on Communications*, Kingston, Ontario, pp. 271–275, May 1994.

[10] F. Patenaude, *Timing Recovery for Continuous Phase Modulation Transmitted over Fast Flat-Fading Channels*, M.A.Sc. Thesis, Ottawa-Carleton Institute for Electrical Engineering, August 1990.

[11] J. H. Lodge and D. Boudreau, "The implementation and performance of narrowband modulation techniques for mobile satellite applications," *Proc. 1986 International Conference on Communications*, Toronto, Ontario, pp. 44.6.1–44.6.7, June 1986.

[12] J. H. Lodge and M. L. Moher, "Maximum likelihood sequence estimation of CPM signals transmitted over Rayleigh flat-fading channels," *IEEE Trans. on Communications*, vol. 38, no.6, pp. 787–794, June 1990.

[13] G. Battail, "Pondération des symboles décodés par l'algorithme de Viterbi," *Annales des Télécommunications*, vol. 42, no. 1–2, pp. 31–38, 1987.

[14] J. Hagenauer and P. Hoeher, "A Viterbi algorithm with soft-decision outputs and its applications," *IEEE Globecom*, Dallas, Texas, pp. 1680–1686, November 1989.

[15] C. Berrou, P. Adde, E. Angui and S. Faudeil, "A low complexity soft-output Viterbi decoder architecture," *IEEE International Communications Conference*, Geneva, pp. 737–740, May 1993.

[16] J. Hagenauer, "Source-controlled channel decoding," *Submitted to the IEEE Trans. on Communications*, April 1993.

[17] D. Boudreau and J. H. Lodge, "A new equalization strategy for the transmission of CPM signals in a fast fading environment," *Proc. 16th Biennial Symposium on Communications*, Kingston, Ontario, pp. 375–378, May 1992.

[18] D. Boudreau and J. H. Lodge, "Adaptive equalization of CPM signals in a fast flat-fading environment," *Proc. 2nd International Conference on Universal Personal Communications*, Ottawa, Ontario, pp. 936–940, October 1993.

[19] D. Boudreau and J. H. Lodge, "Equalization of constant envelope signals based on signal-to-interference ratio optimization," *Submitted to the IEEE Trans. on Communications*, September 1994.

[20] D. Boudreau and J. H. Lodge, "Adaptive equalization of CPM signals transmitted over fast Rayleigh flat-fading channels," *Accepted for publication in the IEEE Trans. on Vehicular Technology*, January 1995.

[21] Y. Jolly, D. Boudreau and J. H. Lodge, "Block-adaptive equalization of CPM signals transmitted over fast flat-fading channels," *Proc. 17th Biennial Symposium on Communications*, Kingston, Ontario, pp. 451–454, May 1994.

[22] D. Boudreau and Y. Viens, "Reduced complexity soft-output maximum likelihood sequence estimation of 4-ary CPM signals transmitted over Rayleigh flat-fading channels," *1995 Canadian Workshop on Information Theory*, Lac Delage, Québec, May 1995.

[23] N. Seshadri and J. B. Anderson, "Decoding of severely filtered modulation codes using the (M, L) algorithm," *IEEE Journal on Selected Areas in Communications*, vol. 7, no. 6, pp. 1006–1016, August 1989.

[24] Y. Li, B. Vucetic and Y. Sato, "Optimum soft-output detection for channels with intersymbol interference," *Submitted to the IEEE Trans. on Communications*, 1994.

UNCLASSIFIED
SECURITY CLASSIFICATION OF FORM
(highest classification of Title, Abstract, Keywords)

DOCUMENT CONTROL DATA

(Security classification of title, body of abstract and indexing annotation must be entered when the overall document is classified)

1. ORIGINATOR (the name and address of the organization preparing the document. Organizations for whom the document was prepared, e.g. Establishment sponsoring a contractor's report, or tasking agency, are entered in section 8.)

COMMUNICATIONS RESEARCH CENTRE
3701 Carling Avenue, P.O. Box 11490, Station H
Ottawa, Ontario K2H 8S2

2. SECURITY CLASSIFICATION (overall security classification of the document. including special warning terms if applicable)

UNCLASSIFIED

3. TITLE (the complete document title as indicated on the title page. Its classification should be indicated by the appropriate abbreviation (S,C or U) in parentheses after the title.)

NARROWBAND TECHNOLOGIES FOR TACTICAL COMMUNICATIONS (U)

4. AUTHORS (Last name, first name, middle initial)

BOUDREAU, DANIEL., JOLLY, YVES., BÉNOIT, PASCAL., BOUCHER, LUC

5. DATE OF PUBLICATION (month and year of publication of document)	6a. NO. OF PAGES (total containing information. Include Annexes, Appendices, etc.)	6b. NO. OF REFS (total cited in document)
JUNE 1995	35	24

7. DESCRIPTIVE NOTES (the category of the document, e.g. technical report, technical note or memorandum. If appropriate, enter the type of report, e.g. interim, progress, summary, annual or final. Give the inclusive dates when a specific reporting period is covered.)

FINAL TECHNICAL REPORT (CRC REPORT # CRC-RP-95-005

8. SPONSORING ACTIVITY (the name of the department project office or laboratory sponsoring the research and development. Include the address.)

DEFENCE RESEARCH ESTABLISHMENT OTTAWA
3701 Carling Avenue, Bldg. 29
Ottawa, Ontario K1A 0Z4

9a. PROJECT OR GRANT NO. (if appropriate, the applicable research and development project or grant number under which the document was written. Please specify whether project or grant)	9b. CONTRACT NO. (if appropriate, the applicable number under which the document was written)
04160 (DFSM-002)	

10a. ORIGINATOR'S DOCUMENT NUMBER (the official document number by which the document is identified by the originating activity. This number must be unique to this document.)	10b. OTHER DOCUMENT NOS. (Any other numbers which may be assigned this document either by the originator or by the sponsor)
CRC REPORT 96-003	

11. DOCUMENT AVAILABILITY (any limitations on further dissemination of the document, other than those imposed by security classification)

(X) Unlimited distribution
( ) Distribution limited to defence departments and defence contractors; further distribution only as approved
( ) Distribution limited to defence departments and Canadian defence contractors; further distribution only as approved
( ) Distribution limited to government departments and agencies; further distribution only as approved
( ) Distribution limited to defence departments; further distribution only as approved
( ) Other (please specify):

12. DOCUMENT ANNOUNCEMENT (any limitation to the bibliographic announcement of this document. This will normally correspond to the Document Availability (11). However, where further distribution (beyond the audience specified in 11) is possible, a wider announcement audience may be selected.)

UNLIMITED

13. ABSTRACT (a brief and factual summary of the document. It may also appear elsewhere in the body of the document itself. It is highly desirable that the abstract of classified documents be unclassified. Each paragraph of the abstract shall begin with an indication of the security classification of the information in the paragraph (unless the document itself is unclassified) represented as (S), (C), or (U). It is not necessary to include here abstracts in both offical languages unless the text is bilingual).

The fundamental building blocks of an implementation of a narrowband mobile radio, using state-of-the-art signal processing algorithms, are presented.

The radio utilizes low bit rate vocoder techniques and bandwidth efficient digital modulation methods.

In order to accomodate challenging design requirements, such as reduced RF channel bandwidth, increased robustness, low transmitted power, and good voice quality, sophisticated signal processing techniques were utilized.

The techniques used in the implementation include combined source and channel coding, efficient adaptive equalization on fading channel, soft-output symbol detection, and combined channel and source coding/decoding. The relationship between the different algorithms is described.

These methods, although computationally extensive, have lead to a very effective narrowband mobile radio transmission scheme.

A prototype radio has been built and tested in real time, under laboratory conditions.

14. KEYWORDS, DESCRIPTORS or IDENTIFIERS (technically meaningful terms or short phrases that characterize a document and could be helpful in cataloguing the document. They should be selected so that no security classification is required. Identifiers, such as equipment model designation, trade name, military project code name, geographic location may also be included. If possible keywords should be selected from a published thesaurus. e.g. Thesaurus of Engineering and Scientific Terms (TEST) and that thesaurus-identified. If it is not possible to select indexing terms which are Unclassified, the classification of each should be indicated as with the title.)

Narrowband Radio
Source and Channel coding
Adaptive Equalization
Soft-Output Symbol Detection
Combined Source and Channel Coding

NO. OF COPIES NOMBRE DE COPIES	COPY NO. COPIE N°	INFORMATION SCIENTIST'S INITIALS INITIALES DE L'AGENT D'INFORMATION SCIENTIFIQUE
1	1	BA
AQUISITION ROUTE FOURNI PAR ▶		CRC
DATE ▶		01 Nov 96
DSIS ACCESSION NO. NUMÉRO DSIS ▶		

DND 1158 (6-87)

National Defence / Défense nationale

#499874

PLEASE RETURN THIS DOCUMENT TO THE FOLLOWING ADDRESS:

DIRECTOR
SCIENTIFIC INFORMATION SERVICES
NATIONAL DEFENCE
HEADQUARTERS
OTTAWA, ONT. - CANADA K1A 0K2

PRIÈRE DE RETOURNER CE DOCUMENT À L'ADRESSE SUIVANTE:

DIRECTEUR
SERVICES D'INFORMATION SCIENTIFIQUES
QUARTIER GÉNÉRAL
DE LA DÉFENSE NATIONALE
OTTAWA, ONT. - CANADA K1A 0K2